Development of out-of-plane instability in rectangular RC structural walls

F. Dashti, R.P. Dhakal & S. Pampanin

Department of Civil Engineering, University of Canterbury, Christchurch

2015 NZSEE Conference

ABSTRACT: Out-of-plane instability is identified as one of the common failure modes of rectangular RC walls. This mode of failure was previously observed in experimental studies of rectangular walls, and has attracted more attention following the observed failure mechanisms of several walls in the recent earthquakes in Chile and Christchurch.

In this study, development of out-of-plane instability in rectangular RC walls and its major sources are scrutinized based on experimental observations as well as on assumptions based on engineering judgment. For this purpose, response of a FEM approach previously verified to be able to capture different failure modes of rectangular walls including out-of-plane instability is used to investigate the steps that lead to this mode of failure in a wall specimen that exhibited out-of-plane instability during testing. Based on this investigation, the parameters that are most likely to govern this mode of failure are identified.

1 INTRODUCTION

According to the observations of the recent earthquakes in Chile and New Zealand, lateral instability of a large portion of a wall section (out-of-plane buckling) was one of the failure patterns that raised concerns about performance of buildings designed using modern codes (Figure 1). Prior to the Chile earthquake, this failure mechanism had only been primarily observed in laboratory tests (Oesterle 1979, Vallenas et al. 1979, Goodsir 1985, Thomsen IV and Wallace 2004, Johnson 2010) (Figure 2). Out-of-plane buckling (also referred to as out-of-plane instability) refers to the (local) buckling of a portion of a wall section out-of-plane, as a result of in-plane cyclic loading with flexural response during an earthquake. The out-of-plane buckling is typically limited to an end region of the wall where vertical tension and compression strains from in-plane cyclic flexure are greatest (Telleen et al. 2012a).

(a) (b)

Figure 1. Out-of-plane instability of rectangular walls: (a) 2010 Chile earthquake (Wallace 2012); (b) 2011 Christchurch earthquake (Elwood 2013).

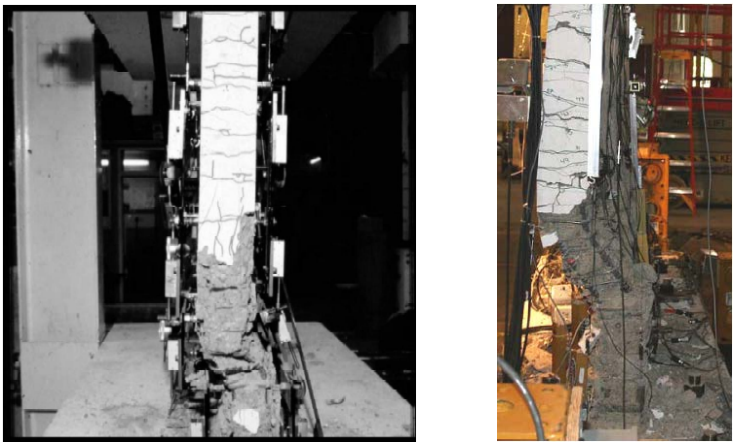

(a) (b)

Figure 2. Wall Out-of-plane instability in laboratory tests: (a) Goodsir (1985); (b) Johnson (2010).

In this study, a FEM approach is used to investigate the steps that lead to out-of-plane instability of rectangular walls. For this purpose, response of a wall model previously verified to be able to capture the out-of-plane instability of walls is used to go over the material behaviour at the section undergoing the maximum out-of-plane displacement.

2 EVOLUTION OF OUT-OF-PLANE INSTABILITY IN RECTANGULAR WALLS

Paulay and Priestley (1993) made recommendations for the prediction of the onset of out-of-plane instability based on the observed response in tests of rectangular structural walls and theoretical considerations of fundamental structural behaviour. Because of very limited available experimental evidences, engineering judgement was relied on extensively; it was concluded that properties for inelastic buckling are more affected by wall length than by unsupported height and the major source of the instability was postulated to be the previously experienced tensile strain than maximum compression strain. Chai and Elayer (1999) studied the out-of-plane instability of ductile RC walls by idealizing the end-region of the wall as an axially loaded reinforced concrete column, as shown in Figure 3, and conducted an experimental study to examine the out-of-plane instability of several reinforced concrete columns that were designed to represent the end-regions of a ductile planar reinforced concrete wall under large amplitude reversed cyclic tension and compression.

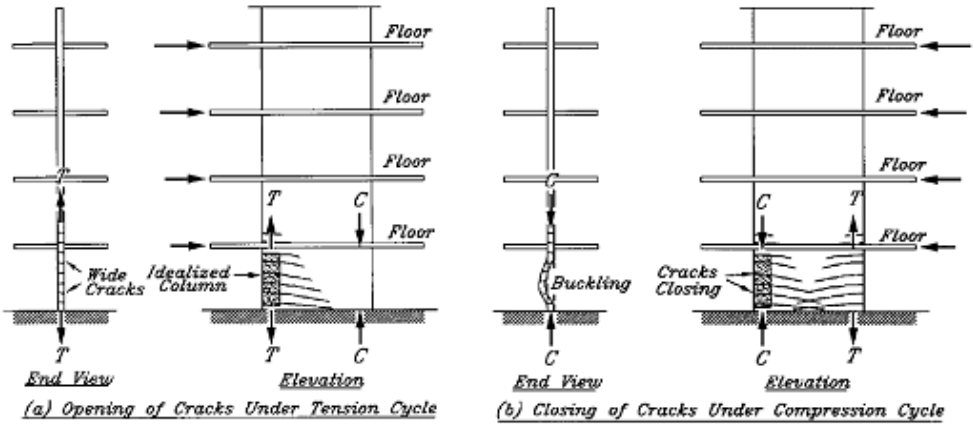

Figure 3. Idealization of reinforced concrete wall in end regions: (a) opening of cracks under tension cycle; and (b) closing of cracks under compression cycle (Chai and Elayer 1999).

Based on this study, the critical influence of the maximum tensile strain on the lateral instability of slender rectangular walls was confirmed and the basic behaviour of the wall end-regions under an axial tension and compression cycle was described by axial strain versus out-of-plane displacement and axial strain versus axial force plots shown in Figure 4. Also, based on a kinematic relation between the axial strain and the out-of-plane displacement, and the axial force versus the axial strain response, a model was developed for the prediction of the maximum tensile strain. Points *a-f* display different stages of the idealized column response and are briefly described in Table 1.

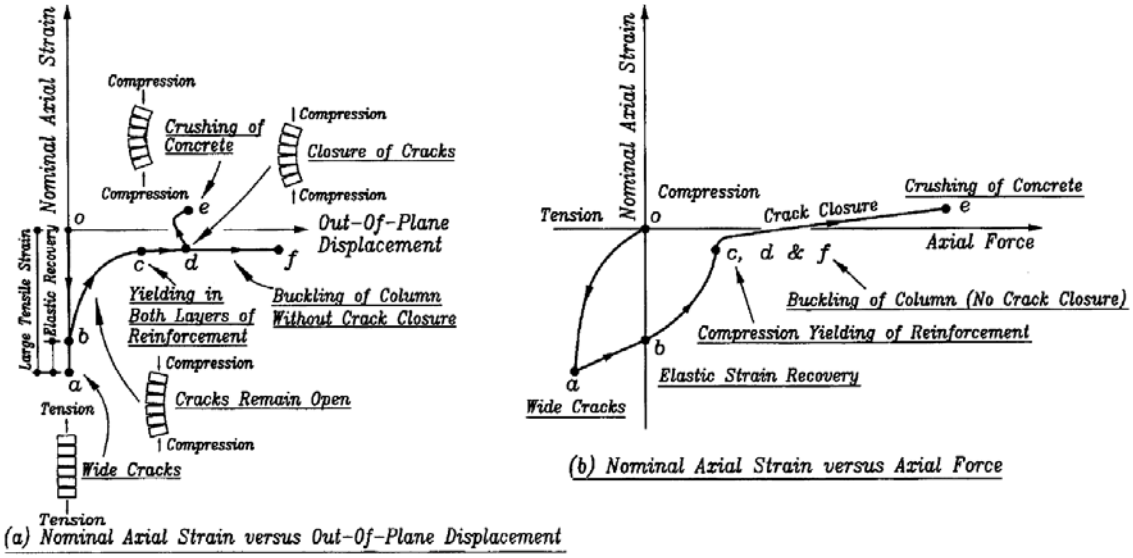

Figure 4. Axial reversed cyclic response of reinforced concrete column: (a) nominal axial strain versus out-of-plane displacement; and (b) nominal axial strain versus axial force (Chai and Elayer 1999).

Table 1. Behavior of wall end-region under the loading cycle shown in Figure 4

	Loading	Unloading	Reloading			
Path	**o-a**	**a-b**	**b-c**	**c-d**	**d-e**	**d-f**
	Large tensile strain	Elastic strain recovery mainly in reinforcing steel	Reloading in compression on the cracked concrete column accompanied by an out-of-plane displacement; yielding of the reinforcement closer to the applied axial force resulting in a reduced transverse stiffness of the column and an increased out-of-plane displacement.	Compression yielding in the second layer of the reinforcement, and a rapid increase in the out-of-plane displacement	Closure of cracks at Point d and decrease of out-of-plane displacement and increase of out-of-plane displacement after significant compressive strain is developed in the compressed concrete	An excessive crack opening where subsequent compression would not result in the closure of the cracks but a continued increase in the out-of-plane displacement and eventual buckling of the column

As can be seen in Figure 4 and Table 1, the idealized column was assumed to consist of the loading stage where a large tensile strain was applied to the specimen (Path *o-a*), the unloading branch (Path *a-b*) corresponding to elastic strain recovery mainly in reinforcement steel and the reloading in compression which can be either Path *b-c-d-e* or Path *b-c-d-f*. During Path *b-c*, when the axial compression is small, the compressive force in the column is resisted entirely by the reinforcement alone as the cracks are not closed, and a small out-of-plane displacement would occur due to inherent eccentricity of the axial force. The increase in axial compression would lead to yielding of the

reinforcement closer to the applied axial force resulting in a reduced transverse stiffness of the column and an increased out-of-plane displacement. Path c-d corresponds to compression yielding in the second layer of the reinforcement due to further increase in the axial compression which could rapidly increase the out-of-plane displacement. Response of the idealized column after Point d depends on the initial tensile strain. If the initial tensile strain is not excessive, the cracks could close at Point *d* resulting in decrease of out-of-plane displacement (Path *d-e*). The crack closure would cause significant compressive strain to develop in the compressed concrete accompanied by increase of out-of-plane displacement. In case of excessive crack opening, the following compression would not be able to close the cracks before the increase in the out-of-plane displacement results in eventual buckling of the column.

3 NUMERICAL MODEL AND PREDICTED RESPONSE

In order to numerically investigate the sequence of material response in a wall section undergoing out-of-plane instability, a FEM model is developed within DIANA9.4.4 (DIANA 2011). Curved shell elements with embedded bar elements are used to simulate the reinforced concrete section. The *Total Strain Crack* model available in DIANA (DIANA 2011) is used to represent the behavior of the concrete elements. The axial stress-strain data captured using Popovics/Mander`s constitutive model (Mander et al. 1988) is implemented in the *Total Strain Rotating Crack* model to incorporate the confined concrete properties in the boundary elements and the behavior of the unconfined portion is modeled using the axial stress-strain relationship of unconfined concrete (Mander et al. 1988). The stress-strain curve of the reinforcing steel is defined using Menegotto and Pinto (1973) model.

The modelling approach has previously been calibrated and verified using experimental results of walls with different shear-span ratios which failed in different modes (Dashti et al. 2014a). Furthermore, experimental results of a cantilever wall specimen (Specimen R2, Oesterle (1976)) which failed in out-of-plane mode were used for verification of the modelling and analysis capability in capturing this mode of failure (Dashti et al. 2014b). Figure 5 indicates properties of the specimen and Figure 6 displays comparison of the numerical simulation with experimental measurements as well as the out-of-plane deformation pattern predicted by the model. This specimen is used in this study to scrutinize the evolution of out-of-plane instability in the numerical model. The wall model was subjected to a relatively large lateral displacement to generate a considerable tensile strain in the boundary region reinforcement and a loading reversal up to a significant drift level in the opposite direction to impose compression on the boundary region that had previously experienced a large tension.

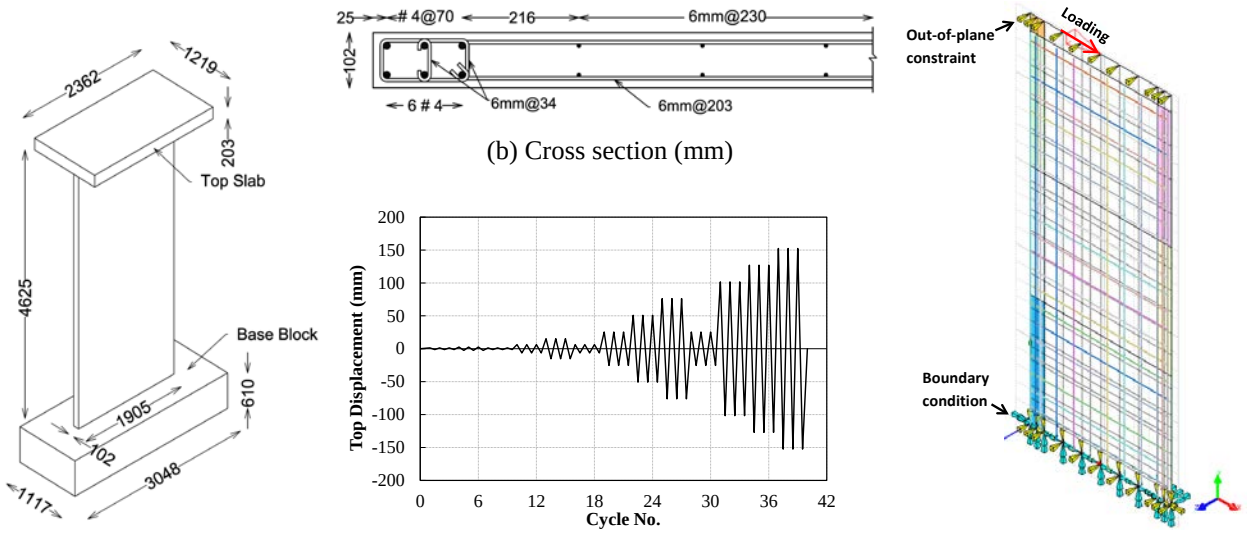

(a) Dimensions (mm) (b) Cross section (mm) (c) Loading history (d) Finite element model

Figure 5. Wall specimen R2 (Oesterle 1976).

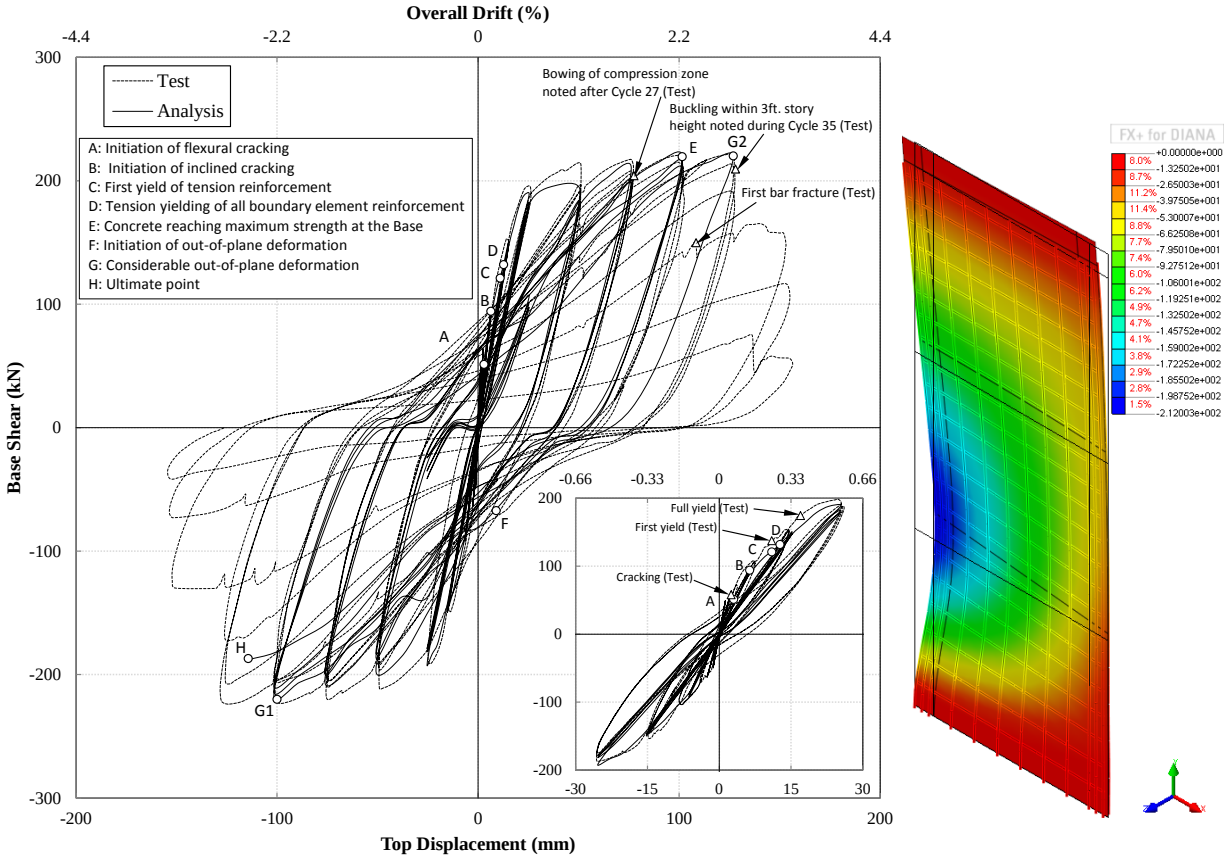

Figure 6. Response of the model: (a) lateral load vs top displacement response and comparison with experiential results; (b) out-of-plane deformation corresponding to Point *H* (ultimate point).

The initial displacement was increased at each attempt trying to capture the peak positive drift corresponding to the initiation of out-of-plane instability during load reversal. Figure 7a displays the top displacement history applied to the model and its comparison with the experimental measurements, and Figure 7b shows the maximum out-of-plane displacement of the left boundary zone versus top displacement of the model. As can be seen in this figure, the out-of-plane displacement initiated when the model was subjected to negative top displacements, increased up to a certain level, and decreased significantly towards a constant residual out-of-plane displacement until end of loading at -6% drift level.

Figure 8 and Figure 9 display the axial reversed cyclic response of the left boundary region reinforcement for both layers of reinforcement at the section where out-of-plane displacement was greatest. The deformation pattern along the wall thickness is shown graphically in each figure to further clarify the sequence of events (C and T displayed next to stand for the compressive and tensile stresses applied to the reinforcement, respectively). The axial strain versus out-of-plane displacement of the boundary region reinforcement shows the same trend as the one of the idealized column specimens tested by Chai and Elayer (1999) (Figure 4). Points *a*-*d* correspond to the stages defined in Figure 4 and in Table 1. However, Point *e* does not correspond to concrete crushing. Although the model was subjected to -6.0% drift level, the axial strain at Point *e*, as shown in Figure 8 and Figure 9, is only -0.0004 which is far away from the axial strain capacity of the boundary zone confined concrete. In other words, the crack closure starting from Point *d* is completed after the wall has been subjected to a considerably large drift, and the main load carrying capacity of the cracked section was provided by the reinforcement only until the magnitude of axial strain reached zero.

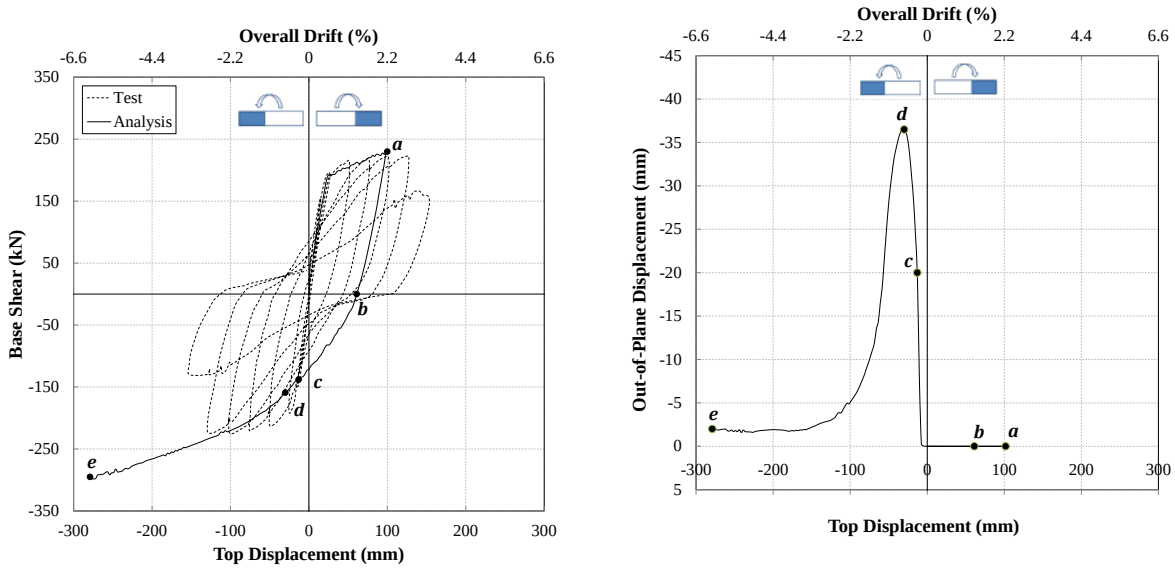

(a) (b)

Figure 7. Response of the model: (a) lateral load vs top displacement response and comparison with experimental results; (b) maximum out-of-plane displacement.

Figure 8 and Figure 9 correspond to different layers of reinforcement. Before initiation of out-of-plane deformation, the strain at two layers of reinforcement is identical (Path *o*-*a* and *a*-*b*) until beginning of out-of-plane deformation during Path *b*-*c* at strain value of 0.0038 (Figure 8 and Figure 9). The reinforcement positioned at the inner face of the deformed section (referred to as Layer 1, Figure 8) undergoes a relatively bigger reloading in compression (recovering to smaller values of strain) for a given out-of-plane deformation when compared to the one at the outer face (referred to as Layer 2, Figure 9), and further reloading results in its compression yielding at Point *c*. As the reloading continues along Path *c*-*d*, compression yielding of the outer layer of reinforcement leads to rapid increase of the out-of-plane displacement. As the initial tensile strain was not big enough, the increase in out-of-plane displacement results in crack closure which in turn decreases the out-of-plane displacement, gradually reducing the difference between the axial strain values of the two layers of reinforcement for a given value of out-of-plane displacement. At Point *e*, the strain values at both layers of reinforcement are almost identical and are negative showing that the crack closure is almost complete with a rather minimal value of out-of-plane displacement.

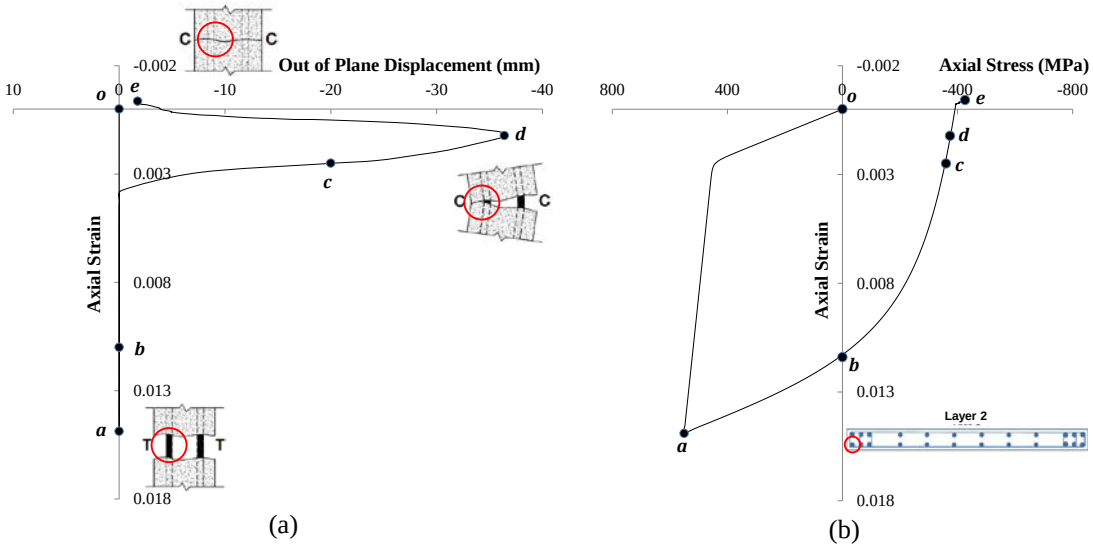

(a) (b)

Figure 8. Axial reversed cyclic response of boundary region reinforcement, Layer1: (a) axial strain versus out-of-plane displacement; and (b) axial strain versus axial stress.

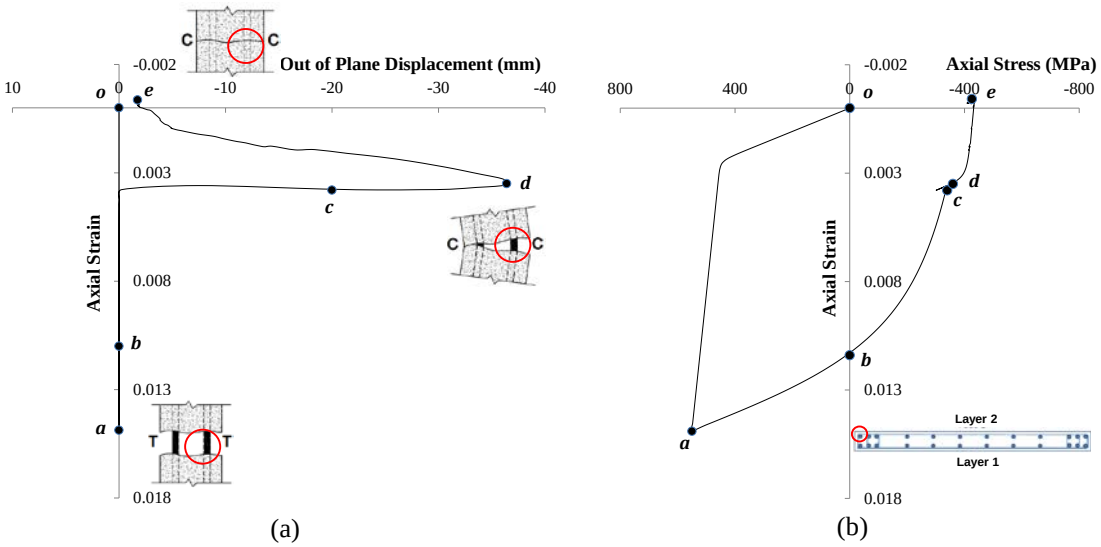

Figure 9. Axial reversed cyclic response of boundary region reinforcement, Layer2: (a) axial strain versus out-of-plane displacement; and (b) axial strain versus axial stress.

The model was subjected to a larger positive displacement to generate larger initial tensile strains in the left boundary region. Figure 10 displays the effect of this loading pattern on the response of the model. As can be seen in Figure 10a, the loading reversal after the model has been subjected to a larger displacement than the previous model resulted in considerable degradation starting from about -2.75% drift. This degradation was due to the considerable out-of-plane deformations of the model which did not recover as the initial tensile strain was big enough to prevent the timely crack closure before the out-of-plane displacement leads to instability of the model. This phenomenon is clearly shown in Figure 11. As shown in this figure, unlike in Figure 8 and Figure 9, the out-of-plane displacement is not recovered along with reloading in compression and the response follows Path *d-f* (Figure 4, Table 1).

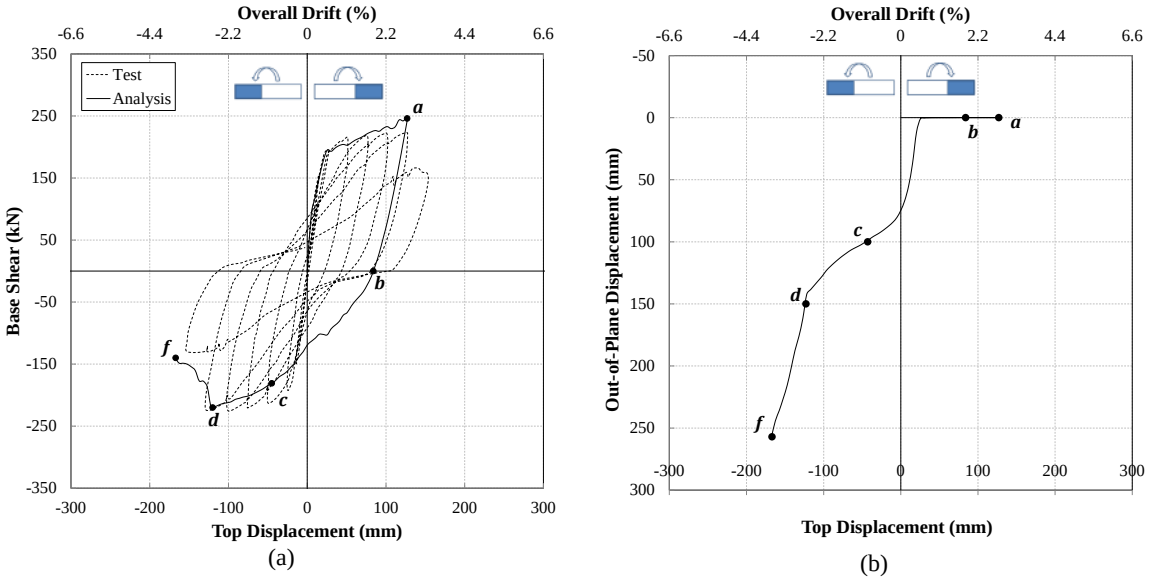

Figure 10. Response of the model: (a) lateral load vs top displacement response; (b) maximum out-of-plane displacement.

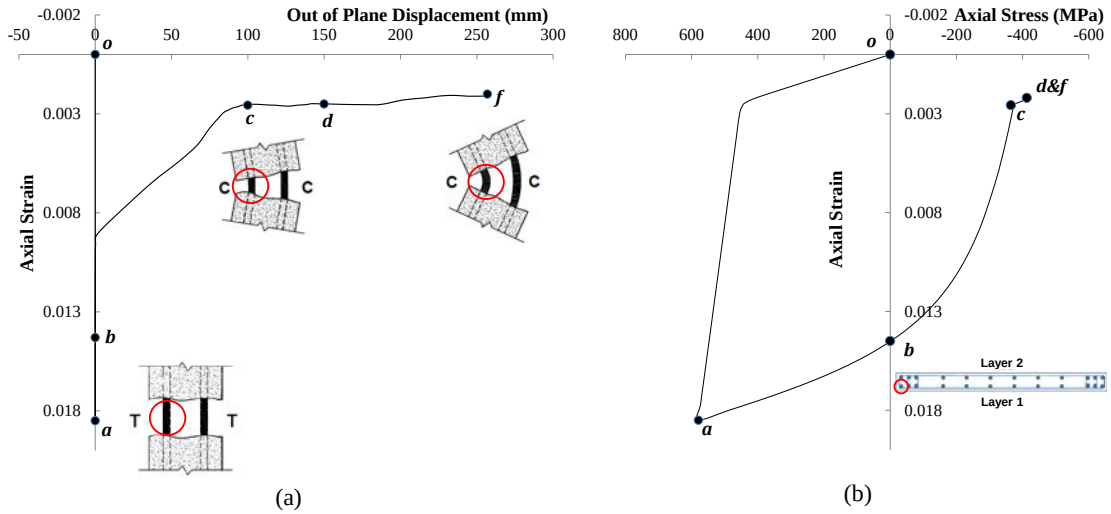

Figure 11. Axial reversed cyclic response of boundary region reinforcement: (a) axial strain versus out-of-plane displacement; and (b) axial strain versus axial stress.

The axial load ratio ($\nu = N/(f'_c A_c)$) is often one of the key parameters affecting failure mechanisms of reinforced concrete structures. In order to investigate the effect of this parameter on the out-of-plane instability of walls, the wall model subjected to the loading history displayed in Figure 7 was subjected to an axial load ratio of 0.1 (corresponding in this case to an absolute value of axial load N=899 kN). The model exhibited a very negligible (almost zero) out-of-plane displacement compared to the one shown in Figure 7b; therefore, the corresponding figures are not presented. Figure 12 displays the effect of axial load on the response of the model. Figure 12b indicates the effect of axial load on the development of axial strain in the boundary region reinforcement. Although the axial load ratio of 0.1 had a negligible effect in the linear elastic stage of the reinforcement, the initially experienced axial strain at loading stage of the model that was subjected to the axial load (Point *a'*) is about 15% smaller than the one without axial load (Point *a*). The axial strain decrease resulting from the applied axial load along the compression reloading path can obviously affect the crack closure and prevent the out-of-plane displacements as the resulting crack opening is smaller than in the case without axial load. It should be noted that the effects of axial load ratio on reinforced concrete structures are complex as it can easily change the failure mode (e.g. from flexure to shear or flexure-out of plane to flexure-concrete crushing), and highly depends on other parameters like shear-span ratio.

On the other hand, the axial load can result in further increase of the out-of-plane displacement if cannot prevent the initial tensile strain from reaching the critical value and the out-of-plane deformation mode initiates, due to the fact that the out-of-plane deformation can readily increase eccentricity of the axial load, producing additional P-Delta effects.

4 PARAMETERS CONTROLLING OUT-OF-PLANE INSTABILITY

Based on the observed response during tests of rectangular structural walls and idealized columns representing boundary regions of such walls as well as on theoretical considerations of fundamental structural behaviour (Paulay and Priestley 1993, Chai and Elayer 1999), the previously experienced tensile strain of the boundary zone reinforcement is considered as the major source of lateral/out-of-plane instability (under in-place loading) of rectangular structural walls. This parameter is important as it controls the crack opening when there is tensile strain applied to the boundary zone. Therefore, any parameter controlling the tensile strain sustained by the boundary region reinforcement can affect the development of an out-of-plane instability mechanism. The wall length is a key parameter governing the strain imposed on the boundary region reinforcement. For a longer wall to reach a given curvature ductility, the strain at the extreme fibres will be greater. The axial load ratio is another parameter that can control the strain profile developed along the wall length. The effects of this parameter in the

elastic range of the material properties seems to be different from those in the inelastic stage when the axial load considerably affects the residual strain developed in the reinforcement and can play a key role as the unloading and reloading of cracked section happens at this stage. Moreover, the axial load can result in further increase of the out-of-plane displacement or prevent its initiation depending on its interaction with the other parameters. The loading protocol, i.e. the number of cycles experienced by the wall at each drift level, can also affect tensile strain of the reinforcement at different stages of loading.

The sequence of events leading to out-of-plane instability of walls scrutinized in the previous section indicates that timely crack closure plays a key role in stability of walls after initiation of the out-of-plane displacements. In addition to the tensile strain experienced in the previous cycles, the wall thickness can control this behaviour as for a given out-of-plane displacement, crack closure will occur sooner for thicker walls. Based on equilibrium equations proposed by Paulay and Priestley (1993) for a section that has exhibited out-of-plane displacement, the length over which this phenomenon is more probable to happen also affects this mechanism and is dependent on the wall height. This parameter and wall thickness are usually catered for as the slenderness ratio.

Ultimately, wall length, height to thickness (slenderness) and axial load ratio are identified by this study as the main parameters governing the wall instability which need to be taken into account into a parametric study, currently undergoing as part of a larger research campaign, to define the range of key parameters affecting/triggering different failure mechanisms in reinforced concrete walls. More information on preliminary results of such parametric study will be reported in future publications.

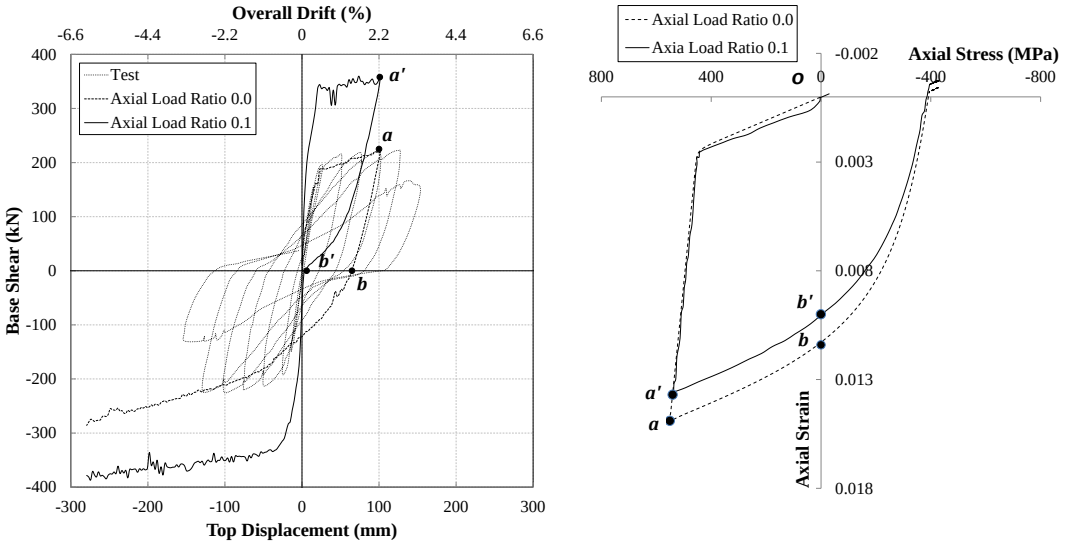

Figure 12. Effect of axial load on response of the model: (a) axial versus top displacement; and (b) axial strain versus axial stress of the boundary region reinforcement.

5 CONCLUSIONS

Development of out-of-plane instability in rectangular RC walls and its major sources were scrutinized in this study considering the investigations found in literature and based on numerical simulations carried out by the authors. For this purpose, response of a FEM approach, previously verified as to be able to capture different failure modes of rectangular walls including out-of-plane instability, was used to investigate the steps that lead to this mode of failure in a wall specimen that exhibited out-of-plane instability during testing under in-plane cyclic loading.

Based on postulations given on stability of structural walls, experimental investigations of idealized columns typifying wall boundary regions as well as scrutinizing section response in a numerical model representing a specimen that had exhibited out-of-plane instability in the lab, the tensile strain imposed

on a reinforced concrete wall should be recognized as a critical parameter governing the lateral stability of the wall. The magnitude of the tensile strain must be such that crack closure, and the subsequent crushing limit state, can be reached.

Any parameter affecting the tensile strain and timely crack closure of the sections undergoing compression reloading can influence the out-of-plane instability of walls.

Wall length, height to thickness (slenderness) ratio and axial load ratio are identified by this study as the main parameters governing the wall instability which need to be taken into account in a parametric study, currently undergoing.

The effects of axial load ratio seem to be different depending on whether the material properties are in the elastic range or in the inelastic stage. In the latter case, in fact, the axial load considerably affects the residual strain developed in the reinforcement and can play a key role as the unloading and reloading of cracked section happens at this stage. Moreover, the axial load can result in further increase of the out-of-plane displacement or prevent its initiation depending on its interaction with the other parameters.

6 REFERENCES

Chai, Y. & Elayer, D. 1999. Lateral stability of reinforced concrete columns under axial reversed cyclic tension and compression. *ACI Structural Journal,* 96(5).

Dashti, F., Dhakal, R. & Pampanin S. 2014a. Numerical simulation of shear wall failure mechanisms. 2014 NZSEE Conference, Auckland, New Zealand, New Zealand Society for Earthquake Engineering.

Dashti, F., Dhakal R.P. & Pampanin S. 2014b. Simulation of out-of-plane instability in rectangular RC structural walls. Second European Conference on Earthquake Engineering and Seismology. Istanbul, Turkey.

DIANA, T. 2011. Finite Element Analysis User's Manual - Release 9.4.4, TNO DIANA.

Elwood, K.J. 2013. Performance of concrete buildings in the 22 February 2011 Christchurch earthquake and implications for Canadian codes 1. *Canadian Journal of Civil Engineering,* 40(3): 1-18.

Goodsir, W.J. 1985. The design of coupled frame-wall structures for seismic actions, University of Canterbury. PhD.

Johnson, B. 2010. Anchorage detailing effects on lateral deformation components of R/C shear walls, Master Thesis, University of Minnesota.

Mander, J., Priestley, M.N. & Park, R. 1988. Theoretical stress-strain model for confined concrete. *Journal of structural engineering,* 114(8): 1804-1826.

Menegotto, M. & Pinto, P. 1973. Method of Analysis for Cyclically Loaded Reinforced Concrete Plane Frames Including Changes in Geometry and Non-elastic Behavior of Elements Under Combined Normal Force and Bending. IABSE Symposium on the Resistance and Ultimate Deformability of Structures Acted on by Well-Defined Repeated Loads, Lisbon.

Oesterle, R. 1976. Earthquake Resistant Structural Walls: Tests of Isolated Walls, Research and Development Construction Technology Laboratories, Portland Cement Association.

Oesterle, R. 1979. Earthquake Resistant Structural Walls: Tests of Isolated Walls: Phase II, Construction Technology Laboratories, Portland Cement Association.

Paulay, T. & Priestley, M. 1993. Stability of ductile structural walls. *ACI Structural Journal,* 90(4).

Telleen, K., Maffei, J., Heintz, J. & Dragovich J. 2012a. Practical Lessons for Concrete Wall Design, Based on Studies of the 2010 Chile Earthquake. 15th World Conference on Earthquake Engineering, 24-28 September 2012, Lisbon, Portugal.

Thomsen IV, J.H. & Wallace, J.W. 2004. Displacement-based design of slender reinforced concrete structural walls-experimental verification. *Journal of structural engineering,* 130(4): 618-630.

Vallenas, J.M., Bertero, V.V. & Popov, E.P. 1979. Hysteretic behaviour of reinforced concrete structural walls. Report no. UCB/EERC-79/20, Earthquake Engineering Research Center, University of California, Berkeley.

Wallace, J. 2012. Behavior, design, and modeling of structural walls and coupling beams—Lessons from recent laboratory tests and earthquakes. *International Journal of Concrete Structures and Materials,* 6(1): 3-18.